

We are IntechOpen, the world's leading publisher of Open Access books Built by scientists, for scientists

6,300

Open access books available

170,000

International authors and editors

185M

Downloads

Our authors are among the

154

Countries delivered to

TOP 1%

most cited scientists

12.2%

Contributors from top 500 universities



WEB OF SCIENCE™

Selection of our books indexed in the Book Citation Index
in Web of Science™ Core Collection (BKCI)

Interested in publishing with us?
Contact book.department@intechopen.com

Numbers displayed above are based on latest data collected.
For more information visit www.intechopen.com



Chapter

Graphene Oxide Based on Biomass Waste: Synthesis and Applications

Ramli Ramli and Rahmat Hidayat

Abstract

Graphene oxide is a two-dimensional material formed from oxidized graphite, with oxygen (O) functional groups decorating the sp^2 plane of carbon (C). Graphene oxide can be obtained by exfoliating the graphite oxide (oxidized three-dimensional carbon-based material) into the layered sheets by sonication or mechanical stirring. Graphene oxide contains various reactive oxygen functional groups, which make it to be a good candidate as a foundation in many applications, such as polymer composites, materials for energy conversion, environmental applications, sensors, FET transistors, and photonic applications, due to its excellent electrical, mechanical, and thermal properties. The widely used technique to synthesize graphene oxide is the modified Hummer's method because of its simple process, low cost, and high yield. In this chapter, we report the progress of graphene oxide synthesis using graphite from activated carbon gathered from biomass waste as the source instead of commercial graphite. The chapter covers the synthesis of biomass waste-based graphene oxide and future perspective applications of graphene oxide. Scientific reports about biomass waste-based graphene oxide synthesis and recent applications of graphene oxide will be discussed. The main motivation for writing this chapter is to bring to the horizon the utilization of biomass waste as an alternative carbon source for the green, low-cost, and sustainable production of graphene oxide.

Keywords: biomass waste, activated carbon, graphene oxide, Hummer's method

1. Introduction

Graphene oxide (GO) is a sheet of graphite oxide obtained by exfoliating graphite oxide into a layered sheet that contains only one or a few layers of carbon atoms through sonication or mechanical stirring [1]. GO can be reduced partially to graphene-like sheets by removing oxygen-containing groups through the restoration of conjugated structure referred to as reduced GO (rGO). These rGO sheets are usually considered to be one type of chemically derived graphene that has similar properties to pure graphene. Graphene and GO are very different, where graphene consists only of sp^2 hybridized carbon atoms, while GO has a carbon structure that is decorated by various oxygen functional groups.

The study of GO was reported in 1859 when the English chemist Brodie named it graphite acid or graphite oxide [2], which was prepared by chemical treatment of graphite with potassium chlorate ($KClO_3$) and nitric acid (HNO_3). After the graphite oxide has been prepared, GO can be obtained by exfoliating the graphite oxide into

monolayer sheets through various thermal and mechanical methods [3]. At present, the single-atom carbon layer of graphite oxide is considered graphene oxide (GO).

GO can be produced using inexpensive graphite by applying cost-effective chemical methods with simple processes and high yields. Furthermore, GO is highly hydrophilic and can form stable aqueous colloids to facilitate the assembly of macroscopic structures by a simple and low-cost solution process [4]. The conventional way to convert graphite oxide into GO is carried out by mechanically exfoliating the graphite oxide, by sonication of graphite oxide in water or a polar organic medium into completely exfoliated GO flakes [5]. In addition, through mechanical stirring of graphite oxide in water, graphite oxide can also be well exfoliated into GO [6]. The sonication and mechanical stirring methods can be combined together to exfoliate the graphite oxide producing a better efficiency than the individual methods separately.

It has been reported that there are four methods to synthesize GO including the Brodie method [2], Staudenmaier [7], Hummer and their modifications [8, 9], and Tour method [10]. Nowadays, the synthesis of GO by the modified Hummer's method has become the most common technique for its production. In the modified Hummer method, graphite is served as the main precursor for GO synthesis.

Graphite is classified into natural graphite and synthetic graphite which can be produced by heating the hydrocarbon precursors at very high temperatures. Meanwhile, the combustion of biomass waste produces charcoal which consists of a mixture of hydrocarbons that could be applied as graphite precursors using graphitization process in a lower temperature.

GO contains various reactive oxygen functional groups, which makes it a good candidate for use in many applications, such as polymer composites, materials for energy conversion and environmental applications [11], sensors, FET transistors, as well as biomedical applications, due to its excellent electrical, mechanical and thermal properties [12]. In this chapter, the synthesis of biomass waste-based graphene oxide and the application of GO in electronics, optics, optoelectronics, as well as energy conversion and storage will be discussed.

2. Synthesis of graphene oxide from biomass waste

Natural graphite and synthetic graphite have several constraints as the precursors in the production of GO, where the natural sources of graphite are limited in some countries and the production process of synthetic graphite requires extremely high temperatures ($\geq 2500^\circ\text{C}$) and demands utmost high cost [13]. Meanwhile, biomass waste has been widely recommended as a potential precursor material for carbon-based synthesis due to its environmental-friendly characteristic, lower temperature process, abundant availability, geographically wide spreading, and lower cost requirements compared to conventional graphite. Several recent studies have suggested biomass as a very appropriate alternative starting material for preparing valuable carbonaceous materials [14–16].

The following section describes the synthesis of GO conducted by the authors by modifying Hummer's method with activated carbon precursors from oil palm empty fruit bunches (OPEFB), rice husks, and coconut shells.

2.1 The synthesis of GO from oil palm empty fruit bunches (OPEFB)

Graphene oxide synthesis from OPEFB was started out by drying the collected empty fruit bunches for 2 days under the sunlight to reduce the water content.

Subsequently, the raw material is then chopped into small pieces and put into various 50, 60, 100, and 125 ml evaporating dishes and let dry in the oven for 60 min at 100°C to completely remove water content existing in empty fruit bunches. The raw material the heated in the furnace for 30 min at various temperature of 250, 300, 350, and 400°C, to convert the empty bunches into charcoal. Furthermore, the charcoal is crushed using a mortar and pestle to produce charcoal powder and sieved with a 270 mesh filter.

The carbon activation was carried out by adding the charcoal powder into 50 ml NaOH solution and left the mixture for 24 h. The solution was dried using oven at 105°C for 3 h to obtain the activated carbon sample. **Figure 1** shows XRD pattern of the sample where the diffraction peaks (002) and (100) presents at $2\theta = 29$ degree and $2\theta = 46$ degree indicate the sample could be considered as graphite. The obtained sample was used as a graphene oxide precursor using the modified Hummer's method.

The synthesis of graphene oxide was carried out by mixing 1.5 g of activated charcoal from OPEFB, 0.75 g of NaNO₃, and 34.5 ml of H₂SO₄ in an Erlenmeyer and stirring the mixture using a magnetic stirrer with 250 rpm at a temperature of 0–5°C for 20 min. The Erlenmeyer was subsequently put into an ice bath to reduce the temperature and keep stirring for 2 h. KMnO₄ powder was slowly added to the mixture to avoid rapid increase in temperature and explosion. Since 4.5 g of KMnO₄ was successfully added, Erlenmeyer was removed from ice bath and stirring temperature was set into 35°C for 30 min. The process was carried out until the mixture shows a milk chocolate color. Furthermore, 69 ml of distilled water was slowly poured into the mixture using a dropper and kept stirring for 20 min until the solution color turned dark brown with the appearance of bubbles. The oxidation process was terminated by adding 100 ml of distilled water followed by 1.5 ml of H₂O₂ which was indicated by yellow color of the solution. Finally, the solution was diluted by adding 50 ml of distilled water and the graphite oxide sample was gathered. Then, the sample GO was sonicated to peel the graphite oxide into layered graphene oxide. The sample was neutralized by distilled water and centrifuged to separate the precipitate and solvent. The separated precipitate was graphene oxide sample that subsequently dried in the oven to completely remove the water content. The GO sample was confirmed by the characterization instrument. **Figure 2** shows

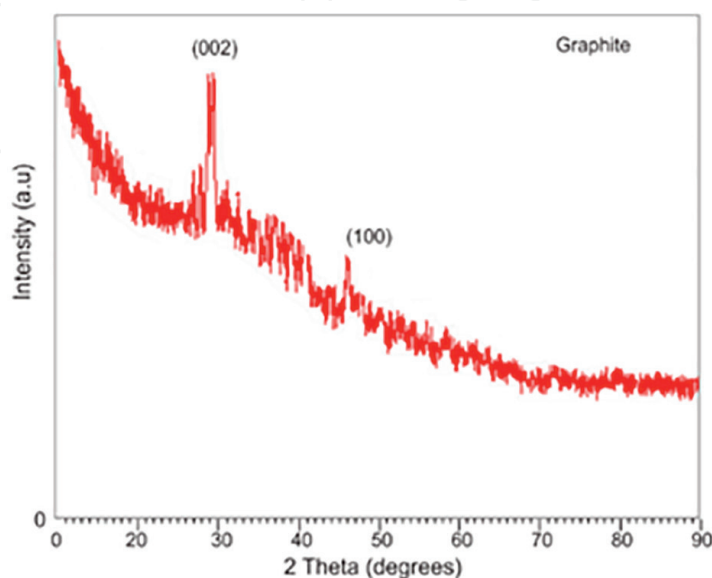


Figure 1.
XRD pattern of activated carbon from (OPEFB).

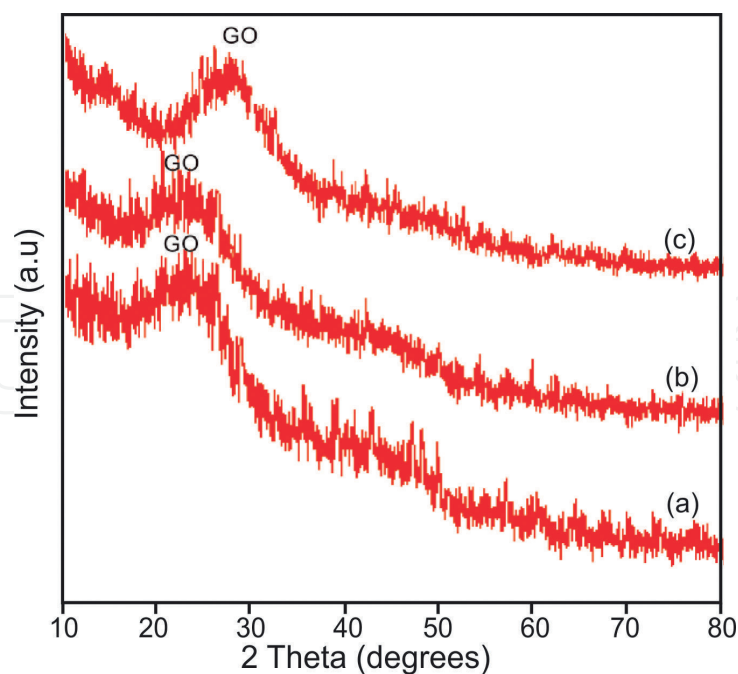


Figure 2. XRD diffraction pattern of graphene oxide from oil palm empty fruit bunches for carbonization temperature (a) 300 °C, (b) 350 °C, and (c) 400 °C.

XRD pattern of OPEFB-based GO. Diffraction peak of the sample appears at angle $2\theta = 26\text{--}29^\circ$ that indicates the structure of graphene oxide.

2.2 The synthesis of GO from rice husk

Rice husk-based GO synthesis began by cleaning the rice husk waste and followed by drying process under sunlight for 3 days. Further drying process was carried out using oven at 105°C for 2.5 h to remove the water and moisture properly. Carbonization process was performed using the furnace for 15 min to produce biocarbon. Various carbonization temperature (250, 300, and 350°C) were used to analyzed the resulted product. Resulted biocarbon was filtered using 140-mesh and 170-mesh sieves to produce uniform particles with a size of $88\text{--}106\ \mu\text{m}$ and prepared as the precursor of synthesis process. Modified Hummers method was applied to fabricate rice husk-based graphene oxide. The process was started by mixing 1 g of as prepared rice husk-based biocarbon, 23 ml sulfuric acid (H_2SO_4), and various masses of sodium nitrate (NaNO_3) in the ice bath and stirred at a speed of 600 rpm for 2.5 h. Various mass of NaNO_3 (0, 0.5, 1, and 2 g) were used. Potassium Permanganate (KMnO_4) with mass of 3 g was slowly add into the mixture by keeping the temperature under 20°C to prevent explosion and stirred for 30 min. After KMnO_4 was completely added, the reaction temperature was raised to 35°C by removing the ice bath and setting the hotplate temperature and stirring process was carried out for 30 min. The mixture was then diluted by slowly adding 46 ml of distilled water and keeping the temperature at $95\text{--}99^\circ\text{C}$ and stirring for 30 min. After the oxidation had taken place, diluted Hydrogen peroxide (H_2O_2) 3% was added to stop the oxidation process and remove the manganese and permanganate residuals. The oxidation process produced rice husk-based graphite oxide and subsequently, the product was exfoliated to produce rice husk-graphene oxide. The solution was set in the Ultrasonic device to perform sonication process. Washing process was performed to neutralize the solution using distilled water and centrifuge for several

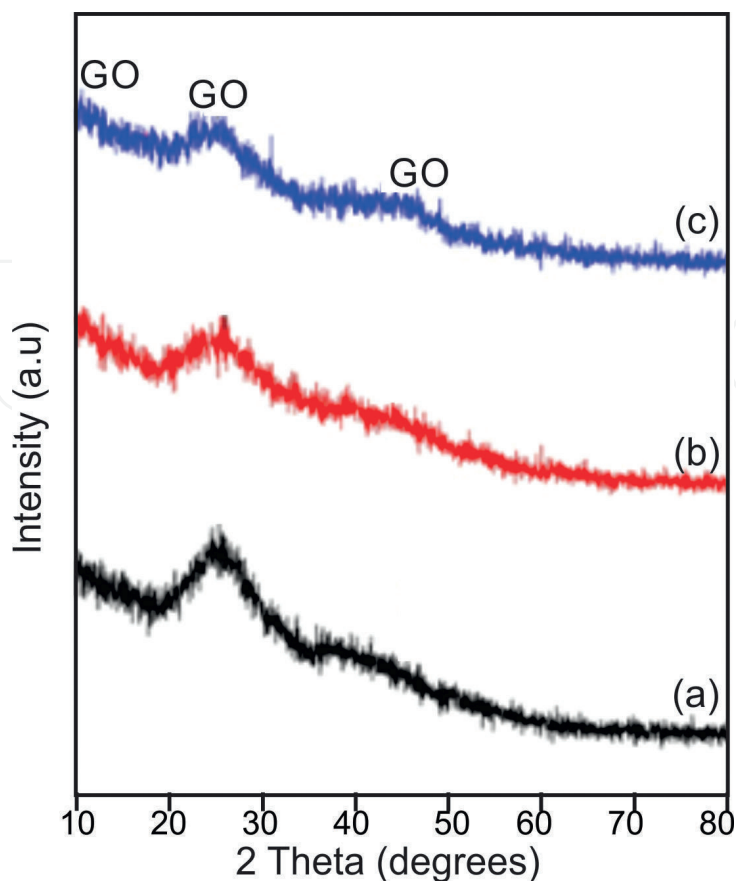


Figure 3. XRD diffraction pattern of graphene oxide from rice husk waste for carbonization temperature (a) 250 °C, (b) 300 °C, and (c) 350 °C.

cycles. When the neutral phase was gathered, the precipitate and liquid were separated. As gathered precipitate was dried in the oven at the temperature of 100°C for 15 min and the rice-husk-based graphene oxide sample was obtained.

The XRD pattern of rice husk-based GO is presented in **Figure 3**. All the variations measured have a fairly identical pattern where the diffraction peak appears at the angle of $2\theta = 10^\circ$ with an interplanar distance of 8.8 Å, at the reflection plane (001), and at the angle of $2\theta = 44^\circ$ with an interplanar distance of 2.1 Å, at the reflection plane (100). These characteristics confirmed the formation of graphene oxide. The diffraction peak at about $2\theta = 22^\circ$ indicates the graphene oxide is not completely bound to oxygen atoms. The diffraction peak at $2\theta = 10^\circ$ indicates the distance between the GO layers, while the diffraction peak around $2\theta = 44^\circ$ indicates the short arrangement of the stack layers GO.

The peak between 26° and 44° indicates the presence of an amorphous solid structure that was formed from natural materials. The change in the peak position was influenced by contained oxygen functional groups, which had oxidized graphite to form GO. This result is in accordance with previous researcher's report that the XRD peak of GO nanoparticles from agricultural waste carbonization appears at the angle of $2\theta = 26.6^\circ$ and $2\theta = 44^\circ$.

2.3 The synthesis of GO from coconut shells

The synthesis process as began by cleaning the coconut shells and drying under the sunlight for 3 days. Dried coconut shell then was cut into small pieces and heated at 100°C for 60 min to completely remove water and moisture content. Carbonization

process of coconut shell was performed using a furnace for 2 h with temperature variations of 250, 300, 350, 400, and 450°C. As gathered coconut shell charcoal was ground and sieved with 125 mesh filter to produce charcoal powder. Subsequently, the charcoal was activated using NaOH solution.

Modified Hummer's method was applied to synthesized coconut shell-based GO. Activated carbon powder from coconut shell with mass of 1.5 g was mixed with 0.75 g Sodium nitrate (NaNO_3) and 34.5 ml of Sulfuric acid (H_2SO_4 98%) an Erlenmeyer and stirred for 20 min at a temperature of 0–5°C at a constant speed of 250 rpm. The Erlenmeyer was then put in an ice bath and 4.5 g KMnO_4 powder was slowly added by considering the temperature of mixture was below 20°C. The Erlenmeyer was removed from the ice bath and the temperature was increased into 35°C and stirred for 30 min to let the oxidation process take place. Distilled water was added to dilute the mixture by volume of 69 ml and stirring process was continued for 20 min and kept the temperature below 50°C. The mixture showed dark brown color with bubbles. In order to terminate the oxidation process 100 ml of deionized water was added and followed by 1.5 ml of 30% H_2O_2 . The appearance of the mixture turned into yellowish color. The mixture was sonicated for 2 h to exfoliate the graphite oxide into GO followed by washing process using distilled water. The solution was precipitated for 1 day until a liquid and solid phases were formed. Separation of the solid and liquid was carried out using a centrifuge at 4000 rpm for 15 min and followed by GO neutralization. After neutral pH was obtained, GO was dried in the oven at a temperature of 60°C for 12 h.

The coconut shell-based GO sample was measured by XRD characterization that presented in **Figure 4**. Diffraction peak of the sample appears at angle $2\theta = 26$ and $2\theta = 29$ degree that signifies the structure of graphene oxide.

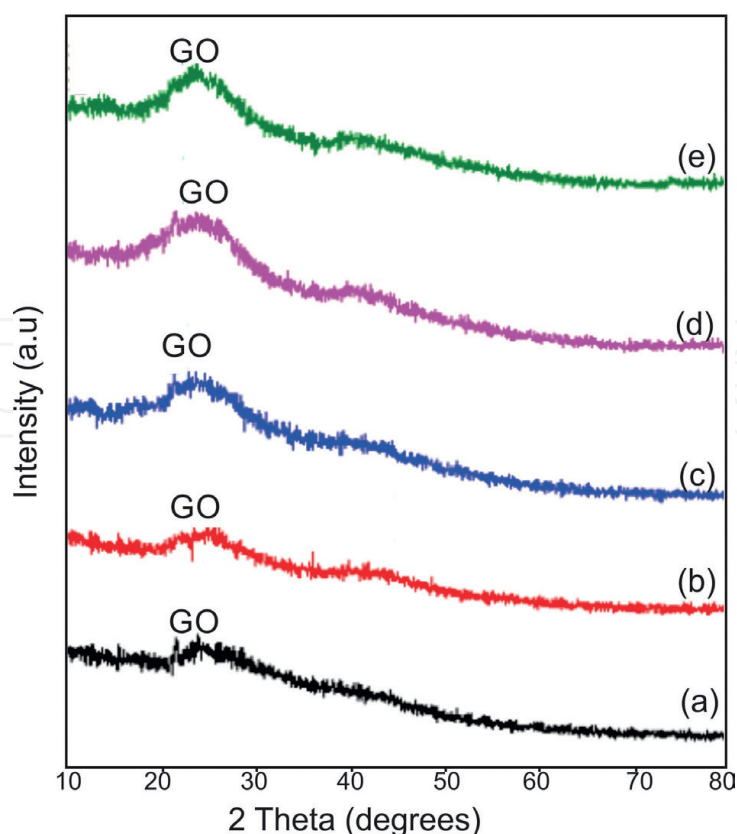


Figure 4. XRD diffraction pattern of graphene oxide from coconut shell for carbonization temperature (a) 250 °C, (b) 300 °C, (c) 350 °C, (d) 400 °C, and (e) 450 °C.

3. Recent application of graphene oxide

Some recent applications of graphene oxide have been found in various devices and prototypes. In the following section, several recent applications of graphene oxide will be described.

3.1 Lithium-ion batteries (LIBs) electrodes

The most widely used power storage in daily gadgets was dominated by a lithium-ion battery which uses graphite material as anode and lithium-based metal oxide as the cathode. GO plays the role in increasing the performance of LIBs by modification of both cathode and anode. GO was added in the fabrication of cathode to modify the property of prior material. The application of GO as additional material in LIBs cathode was found in the manufacture of LiMnPO_4 nano-sized cathodes which has been successfully carried out using the solvothermal method. The role of GO in this synthesis is to cut down the LiMnPO_4 particle size providing a large surface area, and a short diffusion pathway leading to better performance of a lithium battery. The Mn^{2+} ion coordinates with the oxygen functional group on the GO surface to form a small-sized nucleation site of LiMnPO_4 . The particle size of LiMnPO_4 is inversely proportional to the ratio of GO concentration and precursor solution [17]. The presence of LiMnPO_4 on the graphene oxide sheet which is further reduced to reduced GO (rGO) allows a fast electron transfer process between the active material and the collector and accommodates the expansion and contraction of the LiMnPO_4 volume during the charging and discharging process [18, 19]. In addition, GO is also used in the synthesis of $\text{LiMn}_{0.6}\text{Fe}_{0.4}\text{PO}_4$ and $\text{V}_3\text{O}_7 \cdot \text{H}_2\text{O}$ nanorods as the cathode of LIBs. The main role of GO in the synthesis of LIB cathodes is to reduce the particle size so that it reaches nano-size and then GO is reduced using the hydro-/solvothermal method. Apart from being a size reducer, GO is also used to coat cathode materials so as to improve battery performance as found in Vanadium Oxide, LiFePO_4 , $\text{LiNi}_{0.5}\text{Co}_{0.2}\text{Mn}_{0.3}\text{O}_3$ coatings [20, 21].

GO has also been applied intensively in the manufacture of LIBs battery anodes. Although GO plays dominantly as an assistant material in the synthesis process, the virtue of GO properties in the anode manufacturing process cannot be neglected. For example, GO was used in the fabrication of GO-assisted SnO_2 -based anodes in appearance of nanoparticles, quantum dots, spheres and nanorods to improve performance [22–25].

3.2 Lithium sulfur batteries electrodes

The nature of GO which has a high surface area and is rich in oxygen functional groups has been utilized in the manufacture of lithium sulfur battery cathodes. The use of sulfur in battery construction is in consideration of cheap, abundant and non-toxic properties. Unfortunately, Sulfur has some lacks in their property such as low electrical conductivity, and the presence of side products during the charge-discharge process creating obstacles in the use of sulfur in batteries. The aim of GO application in the manufacture of Li-S battery cathodes is to accommodate and inhibit S decomposing Li-Polysulfides and to increase the electrochemical stability of Li-S batteries. GO/S nanocomposites can be synthesized by electrostatic self-assembly method. The negatively charged GO sheet is coated on the positively charged S surface [26–28]. The GO/S composite cathode has a capacity of 950–1400 mAh/g and its performance is stable [29].

Various nano-construction with addition of GO provides better results and impact than without GO. The GO-coated porous carbon-sulfur composite-based cathode

provides a fading capacity rate of up to 0.12% per cycle for up to 400 cycles [30]. The cathode made of GO/S composite wrapped in amylopectin was also analyzed for its performance against the stability of Li-S battery which confirmed good stability [31]. In another study, GO wrapped in hollow sulfur balls with the aid of polyvinylpyrrolidone resulted in 73% retention at 1C after 150 cycles [32]. The GO-wrapped bowl-like sulfur composites were reported to provide free space to accommodate the volume expansion during press cycling [33]. Other GO-based cathodes such as MnO₂-GO [34], cetyltrimethylammonium bromide modified S/GO nanocomposite cathode [35], GO-enclosed walnut-like carbon-based and porous cathode [36], GO and micro-spherical Sulfur composite cathode [37], have been used to increase the performance of Li-S battery with upgrading the capability rate and cycle performance. GO plays the role in the formation of attractive structure of the cathode, increment of the active material loading, and guarantee structural capability during cycling and capture of polysulfides species. In addition, the use of GO with Li₂S is used for long-life and high rate Li-S batteries which provide a decomposition rate of 0.046% per cycle and a coulombic efficiency of 99.7% for 1500 cycles at 2 C [38].

3.3 Supercapacitor electrodes

Supercapacitor is a high-performance electrochemical energy storage that shows excellent properties such as high-power capability, short charge-discharge period, and long cycle life [39]. The charge stored in the SC is principally based on the accumulation of electrostatic charge at the electrode-electrolyte interface which occurs in the electrical double layer capacitance (EDLC), or Faradaic process on the surface of the pseudo-capacitor electrode [40]. GO with outstanding properties has been used to improve SC performance as both electrode and electrolyte. But in the discussion of this book will be limited to the electrodes.

GO can provide pseudo-capacitance and increase the wettability of the electrode in the electrolyte. GO-based electrodes have a larger capacitance than graphene-based electrodes. This experiment was carried out by making GO and graphene electrodes with a mixture of 87 wt% GO samples and graphene, 10 wt% acetylene black and 3 wt% binder which was pressed into pellets. The GO electrode obtained a maximum specific capacitance of 146 F/g and an energy density of 20.39 Wh/kg [41]. Another experiment was reported that LiCoO₂-based SC as the positive electrode and GO as the negative electrode and asymmetric SC using porous GO on conductive stainless steel presents the energy density of 19.2 Wh/kg on voltage region up to 1.5 V, and retain specific capacitance of 85% after 1500 cycle [42].

GO can also be used as a template for MnO₂ nanosheets to increase the surface area [38] and combined with MnO₂ as electrodes to increase capacitance [43–46]. The oxygen group that functions as an anchor site allows the formation of MnO₂ nanoparticles that adhere to the surface and ends of the GO sheets. This not only creates a large surface area but also prevents the agglomeration of GO and MnO₂. The same thing also happened to GO/Mn₃O₄ thin film composite synthesized by the sheet-by-sheet technique giving a specific capacitance of 344 F/g at 5 mV/s [47]. Furthermore, by using the electrophoretic deposition method, or hydrothermal process or co-precipitation, nickel oxide, nickel sulfide and copper oxide can be affixed to the surface of GO nanosheets for high performance SC, namely specific capacitance and current density of 569 F/g at 5 A/g [48], 800 F/g at 1 A/g [49], 245 F/g at 0.1 A/g [50].

Even though the initial electroactive polymers can provide large pseudo-capacitance, but experience swelling properties during the redox process which reduces the

stability of the cycle [51]. To solve this problem, GO is widely used to functionalize conductive polymers to make high-performance SCs. The synthesis of conductive GO-polymers can usually be carried out by utilizing electrostatic interactions between negative GO and positive micelles [52]. When the surfactant micelles are electrostatically adsorbed on the GO surface, the addition of polymers and monomers allows the monomers to dissolve in the hydrophobic core of the micelles surfactant and further polymerization processes can take place in the micelles core. For example, GO/Polyaniline (PANI) was synthesized by in situ polymerization [53–56]. Compositing GO and PANI is possible based on three modes namely (1) $\pi-\pi$ stack (2) electrostatic interactions (3) hydrogen bonding [57]. The GO/PANI hybrid has a high surface area and denser pore volume compared to pure PANI. Which is why this can result in a wider contact area between the PANI nanoparticles and with the electrolyte. Which facilitates the rapid transport of electrolyte ions and electrons to the active site of the composite electrode [58, 59]. The synergistic nature of GO/PANI also enhances cycle stability where the GO width maintains the mechanical deformation during the PANI faradaic process which prevents electrode damage.

3.4 Transparent electrode

Transparent electrodes are needed in a variety of light-based technologies by passing sunlight into the active layer and at the same time served as electrode for current flow. Transparent electrodes widely used today are made of indium material whose supplies have been running low on the earth. In addition, the use of indium-based materials has is not friendly to the environment and the cost for production is high. The use of carbon-based substitute materials gained most attraction of the scientists to develop this technology [60]. Graphene with all of its virtues is on of carbon based the most attractive candidate for development because it has high electrical conductivity and transparency, both of which are requirements for transparent electrodes. Graphene oxide is produced in a series of processes for making graphene-based transparent electrodes which are then reduced to form reduced graphene oxide (rGO).

Fabrication of rGO thin film on a quartz substrate has been carried out by depositing GO solution using spin-coating method. The process was then followed by a reduction to transform GO into rGO. The deposited rGO thin film showed surface resistance of $10^2-10^3 \Omega /sq.$ and transparency reaching 80% at a wavelength of 550 nm [61]. GO film deposition can also be done in a more convenient way. In another study, facile deposition was carried out with colloidal GO which had been mixed with reductant at low temperature and slowly heated causing the GO is reduced and rGO was self-assembled into glass substrate. Additional treatment was performed by irradiate the sample using commercial microwave oven. The sample has electrical properties of 21.97 k $\Omega/sq.$ and optical properties of 30.37% transparency at 550 nm [62].

The transferability of GO to various substrates allows it to be deposited onto flexible substrates. Reduced graphene-based transparent and flexible electrode has applied as moisture sensors attached to human skin. In this case rGO was mixed with polyurethane which gave response and relaxation times of 3.5 and 7 seconds, respectively. This capability does not change when the sensor is stretched to 60% and after 10,000 stretching [63].

3.5 Field effect devices

Amazing electrical conductivity induces the potential of GO to be applied as field effect transistor. Good field emission property and bipolar characteristic of its charge

carrier allows them to be tuned by using gate electrical field [64, 65]. GO with its oxygen group decoration shows improved field emission of the graphene because the charge concentration and type is very sensitive to dopant. Low threshold field emission of <0.1 V/ μm from atomically thin layer of reduced graphene oxide was reported. The edges is decorated by a stable and unique oxygen group of C-O-C bonding from that multiple electron beams are emitted [66].

The field effect emission enables the application of graphene in FET manufacture with more convenient way and low-cost production. Reduced graphene oxide was used to fabricate FET by combination with gold source and dielectrophoresis electrode as drain. When the a backgate voltage was applied, 60% of the devices showed p-type FET behavior, while the remaining 40% showed ambipolar behavior. The experiment was followed by anneal the sample at 200C and giving the result all of ambipolar remains do not change the behavior, meanwhile, the 60% of p-type were change into ambipolar. The maximum charge carrier mobilities in the device are 4.0 cm²/Vs for hole and 1.5 cm²/Vs for electron [67].

Further study reports fabrication of Organic FET using GO that grown on a 100 nm SiO₂ substrate using doped n-type Si as the gate. GO nano layer was distributed on the substrate by spin coating method at 3000 rpm for 40 s. The following steps diluting PMMA on toluene with concentration of 10 mg/ml and deposited to the substrate by spin coating method. The process followed by anneal the samples under nitrogen atmosphere using a hotplate with temperature of 120 C for 15 min. Deposited GO layer served as charge-tunneling layer. Source and drain electrode are next developed by thermal evaporation under 10^{-7} Torr. The performance of Organic FET was analyzed through transfer curves of the sample that shows large gate bias dependent hysteresis with voltage 20 V. After writing an erasing the stored data are well kept with on/off ratio in the order of 10^2 for 10^4 s [68].

3.6 Electrical sensor

Variation of the oxidation degree or adsorbing molecules can affect the electrical characteristic of GO that allowing it applied as electrical sensor [69]. Reduced GO was found in the fabrication of high-performance molecular sensor by deposit it into substrate to form ultrathin continuous network. The GO film was tunably reduced by varying the exposure time of reductant vapor and reduced GO can served as sensor because of change of conductance after molecular adsorption [70]. GO-based sensor shows lower frequency noise compared to SWNT-based sensor [71].

Other report shows that conductance of reduced GO sensor is depend on the concentration of dopamine molecule. It was revealed that at the gate voltage (V_g) of -0.6 V, the conductance of reduced GO films deposited on flexible polyethylene terephthalate (PET) substrate and concentration of dopamine is directly proportional. In addition, the rGO-based device are able to label-freely detect the hormonal catecholamine molecules and their dynamic secretion from living cells [72].

3.7 Flexible electronics

Printed circuit boards face the drawbacks in their use because they cannot be applied to flexible and deformed objects. GO with oxygen functional groups decorating their layers allow it to be deposited onto the various substrates, including flexible substrates. The development of flexible electronics supports the rapid growth of thin, lightweight, and flexible devices. Reduced GO thin films with various thicknesses in

range of one to several layers experiences mechanical flexibility and good electrical conductivity with sheet resistance 43 k Ω /sq. and charge mobility up to 1 and 0.2 cm²/Vs for electron and hole respectively [73].

Another study reports that GO was self-assembled into platelets and exhibit mechanically flexible, macroporous three-dimensional (3D) properties of carbon films with controllable porous size. Use of nitrogen doping (N-doping) of the 3D assemblies of RGO increase electrical properties and high chemical reactivity. The film firstly transferred onto the SiO₂ substrate and further onto flexible PET substrate. The rGO thin film shows sheet resistance of ~128.2 Ω . Further Nitrogen doping decreased the sheet resistances to 13.4 Ω , corresponding to the electrical conductivity of 649 S/cm with the film thickness was 1.15 μ m [74].

3.8 Photovoltaic devices

Since GO can be used as an fabrication of transparent electrodes, the further application was found in more complex devices such as photovoltaic [75], LED [76], and electrochromic devices [77]. Reduced GO was applied in a dye-sensitized solar cell (DSSC) as the transparent electrode and found that sun light can pass through the electrode and the electrons are injected. A device using fluorine tin oxide (FTO) electrode was also fabricated and evaluated with the same procedure for comparison. The result shows that RGO-based device has lower short-circuit current, which can be attributed to the higher sheet resistance and lower transmittance of the RGO [78].

Application of GO have also been reported for organic photovoltaic (OPV) devices where reduced GO served as electrodes. The reduced GO electrodes were deposited on quartz substrates using spin coating of aqueous dispersion of functionalized graphene, followed by a reduction process. Because of the higher sheet resistance, the short-circuit current and fill factor of these rGO-based device are lower than those of control device on ITO [79]. Flexible transparent conductive electrode-based reduced GO for organic photovoltaic (OPV) was fabricated by transferring chemically reduced GO onto PET substrates. When the transmittance of reduced GO is greater than 65%, the device performance mainly relies on the charge transport efficiency through rGO electrodes, but not sensitive to the transmittance. After the tensile strain (~2.9%) was applied on the fabricated OPV device, it can sustain a thousand cycles of bending. Furthermore, the current density of devices can be enhanced by increasing the rGO thickness to lower the sheet resistance, which further improves the overall power conversion efficiency (η), even if the transmittance of RGO film decreases.

3.9 Electrochromic devices

Electrochromic device shows a different appearance in color when some voltage or current was applied. The most widely use of electrochromic device is found on smart glasses, mirrors and windows. Reduced GO/polyaniline (PANI) composite multilayer films were prepared as electrode materials for electrochromic devices to replace conventional indium tin oxide (ITO). The fabrication process carried by deposition of negatively charged graphene oxide (GO) and positively charged PANI upon electrostatic interaction, followed by the reduction of their GO components with hydroiodic acid. The thickness of the multilayer film directly proportional to the number of its bilayers that the thickness of bilayer was about 3 nm. Cyclic voltammetry studies indicated that these thin composite films were electroactive, and their redox reactions were related to the insertion-extraction of counter ions in PANI layers [80].

3.10 Photocatalytic water splitting

Photocatalytic water splitting is an artificial photosynthesis process with photocatalysis material used for the dissociation of water molecules (H_2O) into hydrogen (H_2) and oxygen (O_2), using light. The separation of hydrogen and oxygen molecules was utilized for alternatives hydrogen energy, sterilization, anti-fogging, self-cleaning and air purification.

The electronic property of GO depends on the its constituent element that making GO owing p-type behavior because of oxygen's high electronegativity compared to carbon. Likewise, n-type behavior appears when graphene covalently bonds to electron donating nitrogen-containing functional groups [81].

GO was collaborated with other material to enhance photocatalytic performance. It is reported that high solar photocatalytic H_2 -production activity with reduced GO (RGO)- $Zn_xCd_{1-x}S$ nanocomposite that synthesized by coprecipitation-hydrothermal reduction method. The optimized rGO- $Zn_{0.8}Cd_{0.2}S$ photocatalyst has a high H_2 -production rate of $1824 \mu\text{mol h}^{-1} \text{g}^{-1}$ at the RGO concentration of 0.25 wt% and the apparent quantum efficiency of 23.4% at 420 nm. The addition of GO produces improved photocatalytic hydrogen production by 450% compared with that of the pristine $Zn_{0.8}Cd_{0.2}S$, and better than that of the optimized Pt- $Zn_{0.8}Cd_{0.2}S$ under the same reaction conditions. Reduced GO- $Zn_{0.8}Cd_{0.2}S$ nanocomposite also represents ability to be served as photocatalysts replacing noble metal cocatalysts [82].

3.11 Fuel cell

A fuel cell is an electrochemical conversion device that generates electricity from a redox reaction when supplied with fuel such as hydrogen, natural gas methanol or oxidants such as oxygen, air and hydrogen peroxide. GO is applied in the manufacture of fuel cells to increase the electrocatalytic activity. In addition, GO is also used to make membranes in fuel cells. For example, proton exchange membrane fuel cell (PEMFC) and direct methanol/ethanol fuel cell (DEFC/DMFC).

In addition, GO can be used as an electron donor to reduce precious metal ions without the addition of reductants and surfactants. This causes the growth of metal nanoparticles on the GO surface with high dispersion, uniformity and purity [83]. Noble metals with small sizes that have a large surface area and many angles can show good electrocatalytic abilities in fuel cells. For example, mono-dispersed GO mixed with gold nanoparticles was synthesized by a redox reaction between $AuCl_4$ and GO which resulted in high electrocatalytic activity and electron pathway leading to oxygen reduction reactions. A more interesting result was reported that the 3D GO/carbon sphere supported by silver nanocomposite produced using GO as a reductant showed a significant increase in activity for the oxygen reduction reaction in alkaline media [84]. The 3D structure is useful in driving transport in the catalytic layer and facilitating reactant access to the active site.

GO containing conjugate π bonds were also attractive as a substitute for expensive noble metal materials. The embedding of GO into the polymer matrix can increase the conductivity and reduce membrane fouling. Polymer GO composites can be synthesized by hydrogen bonding and the epoxy ring opening reaction uses amines to form new C-N bonds. Which can function as an active for the electrocatalytic reduction of O_2 to H_2O [85].

4. Conclusions

Graphene oxide is a monolayer of carbon atom decorated by oxygen functional group. Abundant and non-used biomass wastes are promising candidate for carbon source to fabricate graphene oxide due to their highly carbon content. Carbonization process is the key step to produce biomass carbon as precursor. Modified Hummer's method is a facile and simple chemical wet process that can be served to synthesis graphene oxide from biomass waste. XRD pattern showed the Graphene Oxide had successfully produced from biomass waste. Graphene oxide plays important role in the advance science and technology today. GO can be applied as starting material to fabricate electrical and optical device such as cathode of battery and supercapacitor, transparent electrode, field effect device, electrical sensor, flexible electronics, photovoltaic device, electrochromic device, photocatalytic, and fuel cell. Numerous researches continuously report advance application of graphene oxide that depict advance graphene oxide-based technology in the future.

Acknowledgements

The authors would like to thank to Directorate of Research, Technology, and Community Service, Ministry of Education, Culture, Research and Technology of the Republic of Indonesia, through grant: *Penelitian Dasar Kompetitif Nasional*, Contract No. 197/E5/PG.02.00.PT/2022.

Conflict of interest

The authors declare no conflict of interest.

Author details

Ramli Ramli* and Rahmat Hidayat
Nanoscience and Nanotechnology Research Group, Department of Physics,
Universitas Negeri Padang, Padang, Indonesia

*Address all correspondence to: ramli@fmipa.unp.ac.id

IntechOpen

© 2022 The Author(s). Licensee IntechOpen. This chapter is distributed under the terms of the Creative Commons Attribution License (<http://creativecommons.org/licenses/by/3.0>), which permits unrestricted use, distribution, and reproduction in any medium, provided the original work is properly cited. 

References

- [1] Zhao J, Liu L, Li F. Graphene Oxide: Physics and Applications. New York: Springer; 2015. p. 3. DOI: 10.1007/978-3-662-44829-8
- [2] Brodie BC. On the atomic weight of graphite. Philosophical Transactions of the Royal Society of London. Series B, Biological Sciences. 1859;**149**:249-259. DOI: 10.1098/rstl.1859.0013
- [3] Dreyer DR, Park S, Bielawski CW, Ruoff RS. The chemistry of graphene oxide. Chemical Society Reviews. 2010;**39**:228-240. DOI: 10.1039/B917103G
- [4] Ray SC. Applications of Graphene and Graphene-Oxide Based Nanomaterials. Waltham: William Andrew; 2015. p. 39. DOI: 10.1016/C2014-0-02615-9
- [5] Stankovich S, Piner RD, Nguyen ST, Ruoff RS. Synthesis and exfoliation of isocyanate-treated graphene oxide nanoplatelets. Carbon. 2006;**44**:3342-3347. DOI: 10.1016/j.carbon.2006.06.004
- [6] Zhu Y, Stoller MD, Cai W, Velamakanni A, Piner RD, Chen D, et al. Exfoliation of graphite oxide in propylene carbonate and thermal reduction of the resulting graphene oxide platelets. ACS Nano. 2010;**4**:1227-1233. DOI: 10.1021/nn901689k
- [7] Staudenmaier L. *Verfahren zur Darstellung der Graphitsäure* (Method for the preparation of graphitic acid). Berichte der Deutschen Chemischen Gesellschaft. 1898;**31**:1481-1487. DOI: 10.1002/cber.18980310237
- [8] Hummers WS, Offeman RE. Preparation of graphitic oxide. Journal of the American Chemical Society. 1958;**80**:1339. DOI: 10.1021/ja01539a017
- [9] Ranjan P, Agrawal S, Sinha A, Rao TR, Balakrishnan J, Thakur AD. A low cost non-explosive synthesis of graphene oxide for scalable applications. Scientific Reports. 2018;**8**:12007. DOI: 10.1038/s41598-018-30613-4
- [10] Marcano DC, Kosynkin DV, Berlin JM, Sinitskii A, Sun Z, Slesarev A, et al. Improved synthesis of graphene oxide. ACS Nano. 2010;**4**:4806-4814. DOI: 10.1021/nn1006368
- [11] Sierra U, Álvarez P, Blanco C, Granda M, Santamaría R, Menéndez R. Cokes of different origin as precursors of graphene oxide. Fuel. 2016;**166**:400-403. DOI: 10.1016/j.fuel.2015.10.112
- [12] Smith AT, LaChance AM, Zeng S, Liu B, Sun L. Synthesis, properties, and applications of graphene oxide/reduced graphene oxide and their nanocomposites. Nano Materials Science. 2019;**1**:31-47. DOI: 10.1016/j.nanoms.2019.02.004
- [13] Li F, Jiang X, Zhao J, Zhang S. Graphene oxide: A promising nanomaterial for energy and environmental applications. Nano Energy. 2015;**16**:488-515. DOI: 10.1016/j.nanoen.2015.07.014
- [14] Hu BB, Wang K, Wu L, Yu SH, Antonietti M, Titirici MM. Engineering carbon materials from the hydrothermal carbonization process of biomass. Advanced Materials. 2010;**22**:813-828. DOI: 10.1002/adma.200902812
- [15] Miao M, Zuo S, Zhao Y, Wang Y, Xia H, Tan C, et al. Selective oxidation rapidly decomposes biomass-based activated carbons into graphite-like crystallites. Carbon. 2018;**40**:504-507. DOI: 10.1016/j.carbon.2018.09.018

- [16] Bishnu PT, Huimin L, Phillip H, Harry MM, John RD, Sheng D. Low-cost transformation of biomass-derived carbon to high-performing nano-graphite via low-temperature electrochemical graphitization. *ACS Applied Materials & Interfaces*. 2021;**13**:4393-4401. DOI: 10.1021/acsami.0c19395
- [17] Wang K, Wang Y, Wang C, Xia Y. Graphene oxide assisted solvothermal synthesis of LiMnPO₄ nanoplates cathode materials for lithium ion batteries. *Electrochimica Acta*. 2014;**146**:8-14. DOI: 10.1016/J.ELECTACTA.2014.09.032
- [18] Zhao B, Wang Z, Chen L, Yang Y, Chen F, Gao Y, et al. LiMnPO₄/graphene nanocomposites with high electrochemical performance for lithium-ion batteries. *Huagong Xuebao/CIESC Journal*. 2016;**67**(11):4779-4786. DOI: 10.11949/j.issn.0438-1157.20160651
- [19] Jiang Y, Liu R, Xu W, Jiao Z, Wu M, Chu Y, et al. A novel graphene modified LiMnPO₄ as a performance-improved cathode material for lithium-ion batteries. *Journal of Materials Research*. 2013;**28**(18):2584-2589. DOI: 10.1557/jmr.2013.235
- [20] Reddy Channu VS, Ravichandran D, Rambabu B, Holze R. Carbon and functionalized graphene oxide coated vanadium oxide electrodes for lithium ion batteries. *Applied Surface Science*. Jun. 2014;**305**:596-602. DOI: 10.1016/J.APSUSC.2014.03.140
- [21] Yu F, Zhang L, Lai L, Zhu M, Guo Y, Qi P, et al. High electrochemical performance of LiFePO₄ cathode material via in-situ microwave exfoliated graphene oxide. *Electrochimica Acta*. 2015;**151**:240-248. DOI: 10.1016/J.ELECTACTA.2014.11.014
- [22] Zhu YG, Wang Y, Xie J, Cao G-S, Zhu T-J, Zhao X, et al. Effects of graphene oxide function groups on SnO₂/graphene nanocomposites for lithium storage application. *Electrochimica Acta*. 2015;**154**:338-344. DOI: 10.1016/J.ELECTACTA.2014.12.065
- [23] Song H, Li N, Cui H, Wang C. Enhanced capability and cyclability of SnO₂-graphene oxide hybrid anode by firmly anchored SnO₂ quantum dots. *Journal of Materials Chemistry A*. 2013;**1**(26):7558-7562. DOI: 10.1039/c3ta11442b
- [24] Bhaskar A, Deepa M, Ramakrishna M, Rao TN. Poly(3,4-ethylenedioxythiophene) sheath over a SnO₂ hollow spheres/graphene oxide hybrid for a durable anode in Li-Ion batteries. *Journal of Physical Chemistry C*. 2014;**118**(14):7296-7306. DOI: 10.1021/jp412038y
- [25] Reddy MJK, Ryu SH, Shanmugaraj AM. Synthesis of SnO₂ pillared carbon using long chain alkylamine grafted graphene oxide: An efficient anode material for lithium ion batteries. *Nanoscale*. 2016;**8**(1):471-482. DOI: 10.1039/c5nr06680h
- [26] Wu H, Huang Y, Zong M, Ding X, Ding J, Sun X. Electrostatic self-assembly of graphene oxide wrapped sulfur particles for lithium-sulfur batteries. *Materials Research Bulletin*. 2015;**64**:12-16. DOI: 10.1016/j.materresbull.2014.12.036
- [27] Rong J, Ge M, Fang X, Zhou C. Solution ionic strength engineering as a generic strategy to coat graphene oxide (GO) on various functional particles and its application in high-performance lithium-sulfur (Li-S) batteries. *Nano Letters*. 2014;**14**(2):473-479. DOI: 10.1021/nl403404v

- [28] Xiao M, Huang M, Zeng S, Han D, Wang S, Sun L, et al. Sulfur@graphene oxide core-shell particles as a rechargeable lithium-sulfur battery cathode material with high cycling stability and capacity. *RSC Advances*. 2013;**3**(15):4914-4916. DOI: 10.1039/c3ra00017f
- [29] Ji L, Rao M, Zheng H, Zhang L, Li Y, Duan W, et al. Graphene oxide as a sulfur immobilizer in high performance lithium/sulfur cells. *Journal of the American Chemical Society*. 2011;**133**(46):18522-18525. DOI: 10.1021/ja206955k
- [30] Liu S, Xie K, Li Y, Chen Z, Hong X, Zhou L, et al. Graphene oxide wrapped hierarchical porous carbon-sulfur composite cathode with enhanced cycling and rate performance for lithium sulfur batteries. *RSC Advances*. 2015;**5**(8):5516-5522. DOI: 10.1039/c4ra12393j
- [31] Zhou W, Chen H, Yu Y, Wang D, Cui Z, DiSalvo FJ, et al. Amylopectin wrapped graphene oxide/sulfur for improved cyclability of lithium-sulfur battery. *ACS Nano*. 2013;**7**(10):8801-8808. DOI: 10.1021/nn403237b
- [32] Zhang J, Yang N, Yang X, Li S, Yao J, Cai Y. Hollow sulfur@graphene oxide core-shell composite for high-performance Li-S batteries. *Journal of Alloys and Compounds*. 2015;**650**:604-609. DOI: 10.1016/j.jallcom.2015.08.050
- [33] Sun C, Shi L, Fan C, Fu X, Ren Z, Qian G, et al. Bowl-like sulfur particles wrapped by graphene oxide as cathode material of lithium-sulfur batteries. *RSC Advances*. 2015;**5**(36):28832-28835. DOI: 10.1039/c5ra00744e
- [34] Huang X, Shi K, Yang J, Mao G, Chen J. MnO₂-GO double-shelled sulfur (S@MnO₂@GO) as a cathode for Li-S batteries with improved rate capability and cyclic performance. *Journal of Power Sources*. 2017;**356**:72-79. DOI: 10.1016/j.jpowsour.2017.04.065
- [35] Hwa Y, Seo HK, Yuk J-M, Cairns EJ. Freeze-dried sulfur-graphene oxide-carbon nanotube nanocomposite for high sulfur-loading lithium/sulfur cells. *Nano Letters*. 2017;**17**(11):7086-7094. DOI: 10.1021/acs.nanolett.7b03831
- [36] Du X, Zhang X, Guo J, Zhao S, Zhang F. Hierarchical sulfur confinement by graphene oxide wrapped, walnut-like carbon spheres for cathode of Li-S battery. *Journal of Alloys and Compounds*. 2017;**714**:311-317. DOI: 10.1016/j.jallcom.2017.04.258
- [37] Tian Y, Sun Z, Zhang Y, Wang X, Bakenov Z, Yin F. Micro-spherical sulfur/graphene oxide composite via spray drying for high performance lithium sulfur batteries. *Nanomaterials*. 2018;**8**(50):1-12. DOI: 10.3390/nano8010050
- [38] Tian Y, Yu Z, Cao L, Zhang XL, Sun C, Wang D-W. Graphene oxide: An emerging electromaterial for energy storage and conversion. *Journal of Energy Chemistry*. 2021;**55**:323-344. DOI: 10.1016/j.jechem.2020.07.006
- [39] Zhang LL, Zhou R, Zhao XS. Graphene-based materials as supercapacitor electrodes. *Journal of Materials Chemistry*. 2010;**20**(29):5983-5992. DOI: 10.1039/c000417k
- [40] Yang P, Mai W. Flexible solid-state electrochemical supercapacitors. *Nano Energy*. 2014;**8**:274-290. DOI: 10.1016/J.NANOEN.2014.05.022
- [41] Karthika P, Rajalakshmi N, Dhathathreyan KS. Functionalized

- Exfoliated Graphene Oxide as Supercapacitor Electrodes. *Soft Nanoscience Letters*. 2012;2(4):59-66. DOI: 10.4236/snl.2012.24011
- [42] Dighe AB, Dubal DP, Holze R. Screen printed asymmetric supercapacitors based on LiCoO₂ and graphene oxide. *Zeitschrift für Anorganische und Allgemeine Chemie*. 2014;640(14):2852-2857. DOI: 10.1002/zaac.201400319
- [43] Dai K, Lu L, Liang C, Dai J, Liu Q, Zhang Y, et al. In situ assembly of MnO₂ nanowires/graphene oxide nanosheets composite with high specific capacitance. *Electrochimica Acta*. 2014;116:111-117. DOI: 10.1016/j.electacta.2013.11.036
- [44] Chen S, Zhu J, Wu X, Han Q, Wang X. Graphene oxide–MnO₂ nanocomposites for supercapacitors. *ACS Nano*. 2010;4(5):2822-2830. DOI: 10.1021/nn901311t
- [45] Jafta CJ, Nkosi F, le Roux L, Mathe MK, Kebede M, Makgopa K, et al. Manganese oxide/graphene oxide composites for high-energy aqueous asymmetric electrochemical capacitors. *Electrochimica Acta*. 2013;110:228-233. DOI: 10.1016/j.electacta.2013.06.096
- [46] Liu Y, Yan D, Li Y, Wu Z, Zhuo R, Li S, et al. Manganese dioxide nanosheet arrays grown on graphene oxide as an advanced electrode material for supercapacitors. *Electrochimica Acta*. 2014;117:528-533. DOI: 10.1016/j.electacta.2013.11.121
- [47] Gund GS, Dubal DP, Patil BH, Shinde SS, Lokhande CD. Enhanced activity of chemically synthesized hybrid graphene oxide/Mn₃O₄ composite for high performance supercapacitors. *Electrochimica Acta*. 2013;92:205-215. DOI: 10.1016/j.electacta.2012.12.120
- [48] Wu M-S, Lin Y-P, Lin C-H, Lee J-T. Formation of nano-scaled crevices and spacers in NiO-attached graphene oxide nanosheets for supercapacitors. *Journal of Materials Chemistry*. 2012;22(6):2442-2448. DOI: 10.1039/c1jm13818a
- [49] Wang A, Wang H, Zhang S, Mao C, Song J, Niu H, et al. Controlled synthesis of nickel sulfide/graphene oxide nanocomposite for high-performance supercapacitor. *Applied Surface Science*. 2013;282:704-708. DOI: 10.1016/j.apsusc.2013.06.038
- [50] Nicasio-Collazo J, Maldonado J-L, Salinas-Cruz J, Barreiro-Argüelles D, Caballero-Quintana I, Vazquez-Espinosa C, et al. Functionalized and reduced graphene oxide as hole transport layer and for use in ternary organic solar cell. *Optical Materials*. 2019;98:109434. DOI: 10.1016/j.optmat.2019.109434
- [51] Simon P, Gogotsi Y. Materials for electrochemical capacitors. *Nature Materials*. 2008;7(11):845-854. DOI: 10.1038/nmat2297
- [52] Zhang LL, Zhao S, Tian XN, Zhao XS. Layered graphene oxide nanostructures with sandwiched conducting polymers as supercapacitor electrodes. *Langmuir*. 2010;26(22):17624-17628. DOI: 10.1021/la103413s
- [53] Liu Y, Deng R, Wang Z, Liu H. Carboxyl-functionalized graphene oxide–polyaniline composite as a promising supercapacitor material. *Journal of Materials Chemistry*. 2012;22(27):13619-13624. DOI: 10.1039/C2JM32479B
- [54] Xu G, Wang N, Wei J, Lv L, Zhang J, Chen Z, et al. Preparation of graphene oxide/polyaniline nanocomposite with assistance of supercritical carbon dioxide for supercapacitor electrodes. *Industrial and Engineering Chemistry Research*.

2012;**51**(44):14390-14398. DOI: 10.1021/ie301734f

[55] Wang H, Hao Q, Yang X, Lu L, Wang X. Graphene oxide doped polyaniline for supercapacitors. *Electrochemistry Communications*. 2009;**11**(6):1158-1161. DOI: 10.1016/j.elecom.2009.03.036

[56] Luo Z, Zhu L, Zhang H, Tang H. Polyaniline uniformly coated on graphene oxide sheets as supercapacitor material with improved capacitive properties. *Materials Chemistry and Physics*. 2013;**139**(2):572-579. DOI: 10.1016/j.matchemphys.2013.01.059

[57] Wang H, Hao Q, Yang X, Lu L, Wang X. Effect of graphene oxide on the properties of its composite with polyaniline. *ACS Applied Materials & Interfaces*. 2010;**2**(3):821-828. DOI: 10.1021/am900815k

[58] Pendashteh A, Mousavi MF, Rahmanifar MS. Fabrication of anchored copper oxide nanoparticles on graphene oxide nanosheets via an electrostatic coprecipitation and its application as supercapacitor. *Electrochimica Acta*. 2013;**88**:347-357. DOI: 10.1016/j.electacta.2012.10.088

[59] Xu J, Wang K, Zu S-Z, Han B-H, Wei Z. Hierarchical nanocomposites of polyaniline nanowire arrays on graphene oxide sheets with synergistic effect for energy storage. *ACS Nano*. 2010;**4**(9):5019-5026. DOI: 10.1021/nn1006539

[60] Xu Y, Liu J. Graphene as transparent electrodes: fabrication and new emerging applications. *Small*. 2016;**12**(11):1400-1419

[61] Becerril HA, Mao J, Liu Z, Stoltenberg RM, Bao Z, Chen Y. Evaluation of solution-processed reduced

graphene oxide films as transparent conductors. *ACS Nano*. 2008;**2**(3):463-470. DOI: 10.1021/nn700375n

[62] Aimon AH, Hidayat R, Rahmawati D, Sutarto R, Permatasari FA, Iskandar F. Facile deposition of reduced graphene oxide-based transparent conductive film with microwave assisted method. *Thin Solid Films*. 2019;**692**:137618. DOI: 10.1016/j.tsf.2019.137618

[63] Trung TQ, Duy LT, Ramasundaram S, Lee N-E. Transparent, stretchable, and rapid-response humidity sensor for body-attachable wearable electronics. *Nano Research*. 2017;**10**(6):2021-2033. DOI: 10.1007/s12274-016-1389-y

[64] Zhu Y, Murali S, Cai W, Li X, Suk JW, Potts JR, et al. Graphene and graphene oxide: Synthesis, properties, and applications. *Advanced Materials*. 2010;**22**:3906-3924

[65] Novoselov KS, Geim AK, Morozov SV, Jiang D, Zhang Y, Dubonos SV, et al. Electric field effect in atomically thin carbon films. *Science* (80). 2004;**306**(5696):666-669. DOI: 10.1126/science.1102896

[66] Yamaguchi H, Murakami K, Eda G, Fujita T, Guan P, Wang W, et al. Field emission from atomically thin edges of reduced graphene oxide. *ACS Nano*. 2011;**5**(6):4945-4952. DOI: 10.1021/nn201043a

[67] Joung D, Chunder A, Zhai L, Khondaker SI. High yield fabrication of chemically reduced graphene oxide field effect transistors by dielectrophoresis. *Nanotechnology*. 2010;**21**(16):165202

[68] Kim T-W, Gao Y, Acton O, Yip H-L, Ma H, Chen H, et al. Graphene oxide nanosheets based organic

field effect transistor for nonvolatile memory applications. *Applied Physics Letters*. 2010;**97**:0233101-0233103. DOI:10.1063/1.3464292

[69] Jung I, Dikin DA, Piner RD, Ruoff RS. Tunable electrical conductivity of individual graphene oxide sheets reduced at 'low' temperatures. *Nano Letters*. 2008;**8**(12):4283-4287

[70] Robinson JT, Perkins FK, Snow ES, Wei Z, Sheehan PE. Reduced graphene oxide molecular sensors. *Nano Letters*. 2008;**8**(10):3137-3140. DOI: 10.1021/nl8013007

[71] Robinson JA, Snow ES, Bădescu ȘC, Reinecke TL, Perkins FK. Role of defects in single-walled carbon nanotube chemical sensors. *Nano Letters*. 2006;**6**(8):1747-1751

[72] Lin Y-M, Avouris P. Strong suppression of electrical noise in bilayer graphene nanodevices. *Nano Letters*. 2008;**8**(8):2119-2125. DOI: 10.1021/nl080241l

[73] Eda G, Fanchini G, Chhowalla M. Large-area ultrathin films of reduced graphene oxide as a transparent and flexible electronic material. *Nature Nanotechnology*. 2008;**3**(5):270-274

[74] Lee SH, Kim HW, Hwang JO, Lee WJ, Kwon J, Bielawski C, et al. Three-dimensional self-assembly of graphene oxide platelets into mechanically flexible macroporous carbon films. *Angewandte Chemie*. 2010;**122**(52):10282-10286. DOI: 10.1002/ange.201006240

[75] Su Q, Pang S, Alijani V, Li C, Feng X, Müllen K. Composites of graphene with large aromatic molecules. *Advanced Materials*. 2009;**21**(31):3191-3195

[76] Wu J, Agrawal M, Becerril HA, Bao Z, Liu Z, Chen Y, et al. Organic

light-emitting diodes on solution-processed graphene transparent electrodes. *ACS Nano*. 2010;**4**(1):43-48. DOI: 10.1021/nn900728d

[77] Palenzuela J, Vinuales A, Odriozola I, Cabanero G, Grande HJ, Ruiz V. Flexible viologen electrochromic devices with low operational voltages using reduced graphene oxide electrodes. *ACS Applied Materials & Interfaces*. 2014;**6**(16):14562-14567

[78] Wang X, Zhi L, Müllen K. Transparent, conductive graphene electrodes for dye-sensitized solar cells. *Nano Letters*. 2008;**8**(1):323-327

[79] Wu J, Becerril HA, Bao Z, Liu Z, Chen Y, Peumans P. Organic solar cells with solution-processed graphene transparent electrodes. *Applied Physics Letters*. 2008;**92**(26):237

[80] Sheng K, Bai H, Sun Y, Li C, Shi G. Layer-by-layer assembly of graphene/polyaniline multilayer films and their application for electrochromic devices. *Polymer (Guildf)*. 2011;**52**(24):5567-5572. DOI: 10.1016/j.polymer.2011.10.001

[81] Yeh T-F, Chen S-J, Yeh C-S, Teng H. Tuning the electronic structure of graphite oxide through ammonia treatment for photocatalytic generation of H₂ and O₂ from water splitting. *Journal of Physical Chemistry C*. 2013;**117**(13):6516-6524

[82] Zhang J, Yu J, Jaroniec M, Gong JR. Noble metal-free reduced graphene oxide-Zn_xCd_{1-x}S nanocomposite with enhanced solar photocatalytic H₂-production performance. *Nano Letters*. 2012;**12**(9):4584-4589. DOI: 10.1021/nl301831h

[83] Chen X, Wu G, Chen J, Chen X, Xie Z, Wang X. Synthesis of 'clean' and well-dispersive Pd nanoparticles with

excellent electrocatalytic property on graphene oxide. *Journal of the American Chemical Society*. 2011;**133**(11):3693-3695. DOI: 10.1021/ja110313d

[84] Yuan L, Jiang L, Liu J, Xia Z, Wang S, Sun G. Facile synthesis of silver nanoparticles supported on three dimensional graphene oxide/carbon black composite and its application for oxygen reduction reaction. *Electrochimica Acta*. 2014;**135**:168-174. DOI: 10.1016/j.electacta.2014.04.137

[85] Naveen MH, Noh H-B, Al Hossain MS, Kim JH, Shim Y-B. Facile potentiostatic preparation of functionalized polyterthiophene-anchored graphene oxide as a metal-free electrocatalyst for the oxygen reduction reaction. *Journal of Materials Chemistry A*. 2015;**3**(10):5426-5433. DOI: 10.1039/C4TA06774F

IntechOpen